FR II radio galaxies with $z < 0.3$ – II. Beaming and unification

M.J. Hardcastle[1,2][*], P. Alexander[2], G.G. Pooley[2] and J.M. Riley[2]

[1] *Department of Physics, University of Bristol, Royal Fort, Tyndall Avenue, Bristol BS8 1TL*
[2] *Mullard Radio Astronomy Observatory, Cavendish Laboratory, Madingley Road, Cambridge, CB3 0HE*

17 December 2007

ABSTRACT
In a previous paper we presented measurements of the properties of jets and cores in a large sample of FRII radio galaxies with $z < 0.3$. Here we test, by means of Monte Carlo simulations, the consistency of those data with models in which the prominences of cores and jets are determined by relativistic beaming. We conclude that relativistic beaming is needed to explain the relationships between core and jet prominences, and that speeds between 0.5 and $0.7c$ on kpc scales provide the best fits to the data.

Key words: radio continuum: galaxies – galaxies: jets – galaxies: active

1 INTRODUCTION

There is strong and widely accepted evidence for relativistic bulk speeds on parsec scales in radio galaxies and quasars. In the most extreme objects the observed superluminal motions, the rapid variability and consequent high brightness temperatures, and the absence of very strong inverse-Compton emission in the X-ray seem to require relativistic bulk speeds with $\gamma \gtrsim 2$; it seems reasonable to assume that such high bulk Lorentz factors are present close to the active nucleus in all extragalactic radio sources. Evidence that relativistic speeds persist on kiloparsec scales is less conclusive, but in FRII objects a one-sided jet on parsec scales usually connects to a one-sided jet on kiloparsec scales, and the result of Laing (1988) and Garrington et al. (1988) that the brighter jet in an FRII radio source tends to lie in the less depolarized lobe is very hard to explain unless relativistic beaming is still important on these scales.

Relativistic beaming is an essential ingredient in unified models for powerful radio galaxies and quasars (e.g. Barthel 1989); on the assumption that quasars are radio galaxies oriented at less than some critical angle to the line of sight, relativistic bulk speeds in the core and jet imply that the cores and jets of quasars should be more prominent relative to the extended emission and that their jets should be more one-sided. Until recently, the lack of detected jets in FRII radio galaxies, while giving qualitative support to this model, meant that it could not be tested quantitatively.

In a previous paper (Hardcastle et al. 1998; paper I) we discussed the properties of radio jets and cores in a large sample of 3CR FRII radio galaxies with $z < 0.3$ which had mostly been imaged with the NRAO VLA at high resolution and sensitivity. Since there are no quasars in the parent

samples at this low redshift, there is necessarily a population of galaxies in our sample aligned at small angles to the line of sight. We suggested that our results were consistent with a modified version of unified models in which broad-line radio galaxies (BLRG) were the aligned objects and the low-power counterparts of quasars; the jets and cores of the BLRG were systematically more prominent than those of narrow-line radio galaxies (NLRG), and the relative numbers of NLRG and BLRG were consistent with their being divided by a critical angle to the line of sight of $\sim 45°$, similar to that found by Barthel (1989) from the relative numbers of higher-redshift 3CR radio galaxies and quasars. The radio properties of the BLRG in our sample were similar to those of the FRII quasars studied by Bridle et al. (1994). Assuming that relativistic beaming is the dominant factor determining the prominences of the cores, the relationships between the properties of cores and jets implied that the jets were beamed, with characteristic speeds in the jets lower than those in the cores, consistent with the results of Bridle et al. (1994). In this paper we attempt to make this conclusion quantitative by fitting empirical models of relativistic beaming effects to the data derived from the sample.

The observed flux density $S_{\rm obs}$ of a jet with speed $v = \beta c$ and Lorentz factor $\gamma = (1 - \beta^2)^{-\frac{1}{2}}$, emitting isotropically in its rest frame, is related to the flux density that would be observed if it were at rest ($S_{\rm rest}$) by the relation

$$S_{\rm obs} = S_{\rm rest}[\gamma(1 - \beta \cos\theta)]^{-(m+\alpha)} \tag{1}$$

(Ryle and Longair 1967) where θ is the angle made by the velocity vector with the line of sight, α is the spectral index (defined throughout in the sense $S \propto \nu^{-\alpha}$), and m is a constant reflecting the geometry of the beamed component (e.g. Scheuer & Readhead 1979); we use $m = 2$, the value appropriate for a continuous jet. Because in practice the

[*] E-mail *M.Hardcastle@bristol.ac.uk*

material in beams is expected to have a range of speeds, care is necessary in interpreting values of γ and β deduced from this expression as straightforward physical quantities; they nevertheless provide a means of characterising the physical parameters in the beam[†].

The approach to modelling relativistic beaming that we adopt has been widely used in testing unified models of different classes of radio sources (e.g. Scheuer & Readhead 1979; Urry & Schafer 1984; Urry, Padovani & Stickel 1991; Morganti et al. 1995). The prominence of a radio component is defined as the ratio of the flux density of the component to the flux density of the *extended* emission (which we define as the total flux density of the source minus any detected emission from the core and jets). It is assumed that the extended emission is unaffected by beaming; the prominence p' of a beamed component is then taken to be given by the product of some intrinsic prominence p and the Doppler beaming factor given by equation 1;

$$p' = p[\gamma(1 - \beta\cos\theta)]^{-(m+\alpha)} \qquad (2)$$

To see whether observed data are consistent with a particular set of assumptions about the parameters of such a model, we generate large numbers of simulated sources by Monte Carlo methods (assuming an isotropic distribution of angles to the line of sight) and compare the resulting distributions with the observations. By varying the unknown parameters (p and β in this simple model) and examining the goodness of the fit, it is possible to find the values of the parameters that produce simulated datasets that, on average, best reproduce the data (i.e., have the highest probability, on some statistical test, of being drawn from the same parent population). Depending on the fitting statistic used and the space over which it is maximised, this approach may or may not be formally identical to a maximum-likelihood analysis; but in any event we expect it to provide insights into the regions of parameter space suggested by the data.

In the rest of the paper we apply this simple technique to the data of paper I.

2   THE DATA

The sample of paper I consisted of 50 radio galaxies from the samples of Laing, Riley & Longair (1983) and the 3CR catalogue (Spinrad et al. 1991). All had redshifts less than 0.3 and radio power at 178 MHz greater than 1.5×10^{25} W Hz^{-1} sr^{-1}, above the canonical FRI-FRII break (Fanaroff & Riley 1974) although a few had structures which resembled those found in FRIs (e.g. apparently dissipative jets). The reader is referred to paper I for details of the selection criteria. In what follows we assume, as argued in that paper, that the selection was not strongly biased in ways that might affect unified models; in particular, that objects at all angles to the line of sight are represented in the sample.

High-resolution radio maps were available to us for 44 of the 50 objects, and from them we were able to measure

the flux densities of cores and jets and counterjets, or to set upper limits on these quantities where the components were not detected. These quantities, are reproduced from paper I in Table 1. As argued by Bridle et al. (1994), the *straight* component of the jet is the only part in which relativistic beaming effects can usefully be studied, and throughout this paper 'jet flux density' and 'jet prominence' will be used to refer to the flux density and prominence of the straight component of the (brighter) jet only, as defined in paper I. We do not expect to introduce any bias into the data by considering the straight jet only. The prominences of the core and straight jet are also tabulated. If more than one jet is detected in a given source, the prominence of the brighter jet is used; if only one jet is detected, we tabulate its prominence; if no jets are detected, the larger of the two upper limits on jet flux density is used to derive an upper limit on jet prominence. The errors quoted for the fluxes of detected jets are intended to reflect the uncertainty in the separation of the jet from its background, as discussed in paper I, and are not formal errors. Jets or possible jets were detected in 33 of these 44 objects; radio cores were detected in all but 2.

We also tabulate the optical emission-line classes of the sources. We argued in paper I that there is a real difference, in this sample, between the properties of those sources with low-excitation emission lines (low-excitation radio galaxies, LERG) and those with stronger emission lines (the narrow-line radio galaxies, NLRG, and broad-line radio galaxies, BLRG). The prominences of cores and jets for the different classes of object are plotted in Figures 1 and 2. Fig. 2 shows that the most prominent jets are actually those of a subset of the LERG; in paper I we suggested that these were sources with particularly dissipative beams. For this reason we restrict ourselves in what follows to the sub-sample of 31 high-excitation objects.

3   MODEL FITS

Both the distributions of core and jet prominence (plotted in Figs 1 and 2) and the relationship between these quantities (Fig. 3) contain information about the best-fit beaming parameters. It is clear that the distributions could individually be consistent with a relativistic beaming model while exhibiting some relationship (for example, a core-jet prominence anticorrelation) that effectively ruled such a model out. In paper I we showed that both the distributions of these quantities and the positive correlation between them were *qualitatively* consistent with a model in which both cores and jets are relativistically beamed, and with unified models in which the BLRG were the objects more closely aligned with the line of sight. Traditionally the procedure outlined in Section 1 has been applied to a single distribution, e.g. to core prominences (Morganti et al. 1995) or jet sidednesses (Wardle & Aaron 1997). We begin our quantitative approach to the problem in that way; later we discuss the implications of the core-jet relationship.

A serious problem in the data analysis arises because of the number of upper limits in the distributions, particularly in the jet prominences. Whether a jet is apparent in a particular map or not depends not just on the sensitivity of the observations, but also on the presence or absence of confus-

---

[†] As in paper I, we try to follow Hughes & Miller (1991) in distinguishing between the 'beam', the stream of particles supplying the hot spots and lobes with energy, and the 'jet', its observable manifestation.

ing features in the lobe; it is therefore difficult to reproduce the non-detections in the data in numerical simulation. We believe that the upper limits we determine are probably not far above the true values, but in what follows we shall try to assess the effects of the upper limits on the results of the fits.

In order to apply the model discussed in section 1 to a large number of sources, it is necessary to make some assumptions about the intrinsic prominence p of the component of interest. The simplest assumption, adopted by Urry & Schafer (1984) and subsequently followed by other authors, is that the intrinsic prominence of jets or cores is fixed (equivalently, that the intrinsic luminosity of jets or cores is a fixed fraction of the total luminosity of the radio source) so that all sources have the same intrinsic prominence for a given component. This is a reasonable assumption so long as relativistic beaming is expected to be the dominant effect in determining the prominence of a component. In the case of radio galaxies, it seems likely that the environment of, and 'weather' in, a particular radio source can strongly affect the efficiency of jets and cores, and it is certainly true that the environment will affect the *extended* luminosity of a source. The normalisation by extended flux density removes much of the dependence of the prominences of jet and core on the underlying power of the radio source ('beam luminosity') but cannot eliminate it entirely. All of these factors affect component prominences, in general by introducing additional scatter into the distribution of observed prominences. In our analysis we begin by making the simplest assumptions possible, and go on to discuss the effects of relaxing them.

The statistical test we use for comparing real and simulated data throughout the paper is the Kolmogorov-Smirnov (K-S) two-sample test; the statistic provided by this test can be converted to a probability that the two samples compared are drawn from the same parent population [see e.g. Press et al. (1992) for a discussion of the properties and implementation of this test]. We prefer this test to the χ^2 test because of the loss of power involved in binning our small sample; however, wherever we compare two one-dimensional distributions in the following sections we find that the results when a χ^2 test is used are consistent with those of the K-S test.

As discussed in section 2, we believe that the data are not biased with respect to their orientation to the line of sight; this allows us to neglect the details of unified models and to treat the 31 NLRG and BLRG as a homogeneous sample. The clear differences, discussed in paper I, between the core and jet prominences of the BLRG and NLRG motivate the belief that relativistic velocities are involved on both scales; but it would also in principle be possible to use the presence or absence of broad lines as an additional source of information on the inclination of sources in the sample when carrying out model fits. We have chosen not to do this for two reasons: firstly because the presence or absence of broad lines in these objects is strongly dependent on the quality of available optical observations (see e.g. Laing et al. 1994) and because this raises the question of the status of objects in the sample, like 3C 234, with polarized broad lines; secondly because to generate comparison samples requires a knowledge of the critical angle separating the two populations, which, even if such a simple unified model adequately

represents the true situation, is not well constrained, given the small sample size, by the existing data on numbers of sources, supposing the numbers themselves to be accurate. We therefore restrict ourselves, in this section, to noting the degree of agreement between the data and the predictions of a simple unified model (with critical angle 45°) based on our best-fit models.

Throughout the rest of the paper a subscript c denotes a quantity related to the core of a source and a subscript j denotes one related to the jet.

3.1 Cores

Only one of the core prominences for the high-excitation objects is an upper limit (that for 3C 153) and therefore we ignore the problem of upper limits in this part of the analysis, treating the upper limit on 3C 153's core prominence as a measurement. We assume that the spectral index of cores is zero. Because cores are the unresolved bases of jets, which we presume to be intrinsically two-sided, the correct model to use for our sample, where there are angles to the line of sight θ close to 90°, is

$$p'_c = p_c \left\{ [\gamma(1 - \beta_c \cos\theta)]^{-(m+\alpha)} + [\gamma(1 + \beta_c \cos\theta)]^{-(m+\alpha)} \right\} (3)$$

— this is identical to equation 2 at small θ and large β_c, where the second term is negligible in comparison to the first.

Fig. 1 shows the distribution of core prominences in the NLRG and BLRG to be very broad. It is therefore not surprising that when models of the form described in section 1, using the prominence described by equation 3, are fitted to the data only those with large values of β_c can reproduce the data well (Fig. 4). The data do not put an upper constraint on β_c, but they are best reproduced with $\beta_c > 0.95$ (corresponding to $\gamma_c \gtrsim 3$). The lack of an upper constraint is due to the relatively few highly beamed objects in a sample without orientation bias. VLBI information constraining the speeds in the cores is only available for two of our objects: superluminal motion in the core of 3C 111 constrains $\gamma \gtrsim 6.9$ (Preuss et al. 1990) and in 3C 390.3 $\gamma \gtrsim 3.6$ (Alef et al. 1996). Our best-fit Lorentz factors are consistent with these observations. For $\beta_c = 0.98$, under our assumed unified model with a critical angle of 45°, we would expect the median BLRG core prominence in a sample of 31 objects to be about 18 times the median NLRG core prominence, which is larger than the observed ratio of about 8; however, the ratio observed in our data is not inconsistent with this value of the critical angle at the 95 per cent confidence level for any value of β_c allowed by the distribution of core prominences, though it is definitely inconsistent with a critical angle $\lesssim 40°$ unless $\beta_c < 0.98$.

In paper I we discussed a possible positive correlation, only apparent in the narrow-line objects, between core prominence and apparent source linear size. Regression [performed using the Buckley-James method, implemented in the survival analysis software package ASURV Rev. 1.1; LaValley, Isobe & Feigelson (1992)] suggests a non-linear relationship between the two quantities, $p'_c \propto (L \sin\theta)^{1.6\pm0.4}$. This might be attributed to a proportionality between unprojected source length L and *intrinsic* core prominence p_c; such an effect would tend to be seen preferentially in the narrow-line objects, since it would be diluted by projection

and beaming effects in objects at small angles to the line of sight. We may consider two hypotheses:

(i) Intrinsic core prominence is independent of source length; prominences only depend on β_c and θ as in equation 2, and the observed correlation is coincidental.

(ii) Intrinsic core prominence is dependent on source length; prominences depend on β_c, θ and L, the unprojected source length.

In the latter case the core prominence of a source is given by

$$p'_c = k_{c,1} L^a \left\{ [\gamma(1 - \beta_c \cos\theta)]^{-(m+\alpha)} + [\gamma(1 + \beta_c \cos\theta)]^{-(m+\alpha)} \right\} \quad (4)$$

where a governs the relationship between L and p'_c. The effects of projection and beaming will tend to flatten the power-law slope of the observed relationship compared to the true one. The magnitude of this effect, observed in simulated datasets, depends on β_c and the unification angle, but for plausible values of both we expect the observed slope to be flatter than the true slope by about 0.2, so that the true slope a is likely to be about 1.8 ± 0.4. For simplicity, therefore, we choose $a = 2$, a value consistent with the data. $k_{c,1}$ is the constant of proportionality in this relationship and clearly (for this choice of a) has units of kpc^{-2}.

To use Monte Carlo methods to test these models against the data, we first need to model the distribution of unprojected source lengths in the parent population. Little is known about this distribution. The simple empirical form suggested by Kapahi (1976) is not a particularly good fit to our data, as it overpredicts the number of small sources. Simulation shows that the data are moderately well described by a simple normal distribution of unprojected length (mean 560 kpc, standard deviation 230 kpc) with negative lengths being discarded. We use simulated unprojected lengths drawn from this distribution to test the hypotheses.

We first repeated the core prominence simulations to find the best-fit values of $k_{c,1}$ and β_c for model (ii). The results of the simulations for β_c are not strongly affected by the inclusion of a length dependence, presumably because the distribution of core prominences in the data is much broader than that of lengths. Lower values of β_c become slightly more probable, as we would expect (Fig. 5). There is again no constraint on the maximum value of the beaming speed β_c, so we choose a representative value of $\beta_c = 0.98$, corresponding to $k_{c,1} \sim 2.5 \times 10^{-7}\ \mathrm{kpc}^{-2}$. Using these values, we were able to generate pairs of (projected length, apparent core prominence) values to match those in the real dataset. We can then answer the question: how likely is it under the two hypotheses that 22 NLRG cores would produce the significant positive correlation seen on a Spearman Rank test in the real data? Assuming that a critical angle of $45°$ to the line of sight divides broad- and narrow-line objects, and setting the significance level for the one-tailed Spearman-Rank test at 99%, we find that under model (i) only 0.1% of simulated samples could produce such a result, whereas under model (ii) approximately 94% of samples can do so. Model (i) may be rejected at a high level of significance, but model (ii) is consistent with the data. The physical interpretation of this result is unclear.

3.2   Jets

We begin by treating the upper limits on jet prominence as measurements and considering only beaming to be responsible for the distribution of observed jet prominences. We take the spectral index of a jet to be 0.8; the analysis is not significantly affected if this number is altered. The results of the simulations are plotted in Fig. 6. There is a clear best-fit value, corresponding to $\beta_j = 0.62$, $p_j = 0.005$, although again a wide range of parameters is formally acceptable. Assigning a confidence range in the standard way, we find that $\beta_j = 0.62^{+0.04}_{-0.1}$ at the 90 per cent confidence level. For a unified model with critical angle $45°$, we would expect the median BLRG jet with this value of β_j to be about 4 times more prominent than the median NLRG jet; this appears consistent with the distribution seen in Fig. 2, though it is somewhat higher than the ratio (~ 2) of the medians quoted in paper I, where the median jet prominence was calculated on the assumption that all the upper limits fell below the median. The data are better fitted by smaller values of β_j and/or larger critical angles.

If we were able to replace our upper limits with true measurements, we would expect the distribution of jet prominences to broaden, so that the best-fit values of β_j would increase. Although we do not know how far below the upper limits the true measurements lie, we can assess the effect that they have on the results of the fits by allowing them to vary while the fits are being performed. We therefore ran a set of fits in which, at the same time as the comparison population was generated, each of the 7 upper limits present in the data was divided by some factor randomly drawn from a uniform distribution between 1 and 50. The value 50 was chosen as being the ratio between the highest jet prominence upper limit and the lowest actual measurement, though we expect that the difference between the upper limits and the true measurements will usually be less than this. The effect is to increase the best-fit values of β_j, but only slightly; this shows that the effect of the upper limits on our results is not a serious one.

Whereas there is evidence from superluminal motions that relativistic beaming should dominate the prominences of cores, we have little direct evidence that it dominates the prominences of the kpc-scale jets, as discussed in section 1. It is thus worth considering what effect random variation of intrinsic jet prominence (due to 'weather', as discussed above) might have on the best-fit beaming speeds. In general this will reduce the best-fit β_j, because less beaming is required to produce the observed spread in prominences; clearly if the distribution of intrinsic prominence is made to match the observed prominence distribution then no beaming is necessary. A further constraint on prominence distributions is provided, however, by the distribution of jet *sidednesses* in the data; the sidedness of a source is defined, as in paper I, as the ratio of the jet and counterjet prominences. If we assume that the intrinsic prominences of the jet and counterjet are drawn from the same distribution, then we can determine the distribution of sidednesses in a simulated dataset. Because we only have a few counterjet detections in the real dataset most of the sidedness data we have come in the form of lower limits, while we have no constraints at all on the sidedness of the 7 objects where no jet was detected. We therefore incorporate the sidedness constraint by mea-

suring the fraction of the simulated sidednesses that match the measured ones, either by being within $\pm20\%$ of them if they are actual measurements or by being greater than them if they are upper limits. 7 of the simulated sidednesses are allowed to take any value. We then multiply the K-S probabilities of a fit to the prominence data by this fraction to give a (notional) total probability of matching the data. It turns out that for $\beta_j \gtrsim 0.5$ almost all the simulated datasets can match the real dataset's sidedness in this sense; that is, the weighting fraction is 1 for $\beta_j \gtrsim 0.5$ and falls off below it.

Unsurprisingly, then, when we draw the logs of the simulated intrinsic prominences from a normal distribution, which is (as can be seen from Fig. 2) not badly matched to the data, allowing both the mean (p_j) and standard deviation (σ) of the distribution to vary, the best fits are achieved with $\beta_j \sim 0.5$, $\sigma \sim 0.3$ (logs being taken to base 10). However, acceptable fits (probabilities > 0.05) are found for $\sigma \sim 0.4$, $\beta_j \lesssim 0.1$. We cannot use the data on jet prominences and sidednesses alone to rule out a model in which intrinsic jet and counterjet prominences are drawn at random from a sufficiently broad distribution with *no* or negligible relativistic beaming effects. If, however, we make the (perhaps more physically reasonable) stipulation that intrinsic jet and counterjet prominences are the same in particular sources, then the simulations favour the relativistic beaming model more strongly, and the best-fit β_j is higher.

We note finally that it is likely that jets do not emit exactly isotropically in their rest frames; this would affect the beaming relation. Where good polarization measurements are available the magnetic field in FRII jets appears to be directed longitudinally, though it is likely, given that the polarizations of jets are considerably less than the limiting value of ~ 70 per cent, that we are actually seeing a projected, tangled field. In the limiting case of a uniform longitudinal field the correct prominence relation for jets is given by

$$p_j' = p_j[\gamma_j(1 - \beta_j \cos\theta)]^{-(3+2\alpha)}(\sin\theta)^{1+\alpha} \qquad (5)$$

(e.g. Cawthorne 1991), producing a different expected distribution of prominences for a given value of β_j. The increase in the exponent of the Doppler factor and the additional term in $\sin\theta$ to some extent cancel each other's effects. and so the cumulative probability distributions are not actually very different over the whole possible range of θ for the moderate values of β that seem to be appropriate here. When we performed our fits using the prominence relation of equation 5, we obtained very similar best-fit values of β_j but slightly higher values of p_j. If the magnetic field is not uniform and longitudinal, as expected, then our analysis will be even less strongly affected.

3.3 Relations

In Fig. 3 we plot the core and jet prominences for the 31 high-excitation objects in the sample. A correlation is apparent, significant at the 95 per cent level on a modified Spearman Rank test (as implemented in ASURV). As we argued in paper I, if the prominences of cores are dominated by relativistic beaming, such a correlation is not expected unless jets too are beamed; any intrinsic relationship between core and jet would be washed out by the beaming of the cores. But there is clearly substantial deviation from

the predictions of the simplest relativistic beaming models, where intrinsic jet and core prominence are the same for all sources; in such models the points in Fig. 3 would be expected to lie on a single curved line (cf. Bridle et al. 1994) which we plot, for comparison, in Fig. 3. Scatter about this line can arise in a number of ways. It is possible, for example, that there is normally jet bending on 100-pc scales, so that the beaming angle θ is different for core and jet; it is also possible that β_c and β_j vary significantly from source to source. In the simplest models, though, the scatter about the solid line in Fig. 3 has implications for the distribution of intrinsic core and jet prominences, discussed above.

We have already argued that the cores are necessarily beamed, but that the data seem to show a relationship between the intrinsic core prominence and the linear size of the source — a relationship which is not obvious in the jet prominences (see Fig. 5 of paper I). We have seen that jet prominences are well modelled with a combination of intrinsic scatter and beaming. We may now ask whether these two models, when combined, are consistent with the observed relationship between core and jet; and we can try to make quantitative our conclusion that models without beaming in the jets are ruled out by this relationship.

We begin by asking whether the combined models are consistent with the observed correlation found on the Spearman Rank test. Spearman's r for the 31 real data points, as calculated taking limits into account with ASURV, is 0.340. We simulate core and jet prominences based on equations 4 and 2 respectively, drawing the logs of the intrinsic prominences of simulated jets from a normal distribution as in section 3.2 and drawing the lengths of radio sources from the distribution discussed in section 3.1; for cores, as before, we choose $\beta_c = 0.98$. Unsurprisingly, models in which the spread in intrinsic prominence dominates the distribution of jet prominences (so that jet and core are essentially unrelated) cannot adequately reproduce the correlation; if $\beta_j = 0.1$, $\sigma = 0.4$, the probability of obtaining a correlation at least as strong as this is ~ 5 per cent, the level expected to occur by chance, whereas if $\beta_j = 0.5$, $\sigma = 0.3$ it is a more acceptable 75 per cent. We can rule out at the 90 per cent confidence level all the best-fit models for jet prominence derived in section 3.2 that have $\beta_j \lesssim 0.2$, reinforcing our conclusion that beaming is necessary in the jets.

As a final test, we can ask whether the distribution of core and jet prominences in Fig. 3 is consistent with the model we have devised. Peacock (1983) provides a two-dimensional version of the Kolmogorov-Smirnov test, subsequently refined by Fasano & Franchesini (1987); we use the implementation of their test given by Press et al. (1992), though we have verified that the original version of Peacock (1983) gives similar results for our data. Fixing the parameters for the core at $\beta_c = 0.98$, $p_c = 0.05$, we allow the jet β_j and intrinsic prominence to vary; we find, as we expect, that the results are similar to those plotted in Fig. 6. The data are (just) acceptably fitted by a model with no intrinsic scatter, corresponding to the solid line in Fig. 3. However, they are better fitted (K-S probabilities of 50–60 rather than 10 per cent) by models in which there is some dispersion in the intrinsic prominences. If we allow the intrinsic core prominences to depend on length, as above, and the intrinsic jet prominences to be drawn from a normal distribution, then as before the best results are obtained with $\beta_j \sim 0.5$, $\sigma \sim 0.3$.

Models in which the jet and core are uncorrelated (θ_c and θ_j are both randomly chosen rather than being the same) give acceptable but poorer fits to the data, while models in which the jet and core are anticorrelated ($\theta_c = (\pi/2) - \theta_j$) are never acceptable fits, as we would expect.

4　DISCUSSION AND CONCLUSIONS

The results of the previous section allow us to conclude with little ambiguity that relativistic beaming really is significant in determining the prominences of the kpc-scale jets of these objects, providing that it also dominates the prominences of the cores. Speeds between 0.5 and $0.7c$ seem to provide the best fits to the data. Speeds much higher than this do not reproduce the distribution of jet prominences well, while lower speeds cannot well reproduce the observed relationships between core and jet prominence and the jet sidedness distribution, and are in any event at odds with observations of the Laing-Garrington effect. These conclusions are similar to those in earlier work (Bridle et al. 1994; Hough 1994; Wardle & Aaron 1997) but they are based on a sample that should be free of (unknown) orientation bias. Subject to the caveats already discussed, the data and the relativistic beaming speeds derived from them are broadly consistent with the simple unified model of paper I, in which BLRG are aligned at angles less than $\sim 45°$ to the line of sight.

Are these beaming speeds a reflection of any real physical velocity in the beams? As pointed out by Bridle et al. (1994), it is entirely possible that the material in the beam does not move with a single speed. If this is true, the speed derived from a *single* object is, as they say, a weighted average over the velocity field in the beam; the speed derived by application of equation 2 to a whole sample of beamed objects is still more complicated in its relationship to any true physical speeds. Related to this is the whole question of where the jet emission comes from, and why, in fact, we see emission from the beam at all. However, if (as has been suggested; e.g. Bridle 1996) the emission in these objects comes from a shear layer at the edge of the beam, while the emission from a higher-velocity central spine is suppressed to negligible levels by beaming, then the characteristic speeds we derive may well be a reasonable estimator of the physical speeds in the shear layer. Such a picture may also help us to understand why the speeds derived from cores and jets are so different; perhaps we are simply seeing different velocity regimes because different regions of the beam are emitting. Alternatively, it may be that the difference is evidence of a genuine deceleration of the beam between the two scales. Such deceleration is invoked in models of FRI radio sources, where similar speeds around $0.5c$ are derived, from sidedness arguments, at the bases of the jets; [e.g. Hardcastle et al. (1996), Laing (1996), Hardcastle et al. (1997)]. As discussed by Bowman, Leahy & Komissarov (1996) it is possible to decelerate FRII beams by entrainment without excessive dissipation.

Another, related question is raised by the derived intrinsic prominences. The best-fit intrinsic prominences of cores in our sample are $\gtrsim 0.02$, with the value for our representative $\beta_c = 0.98$ ($\gamma_c \approx 5$) being about 0.05. These numbers are similar to those that have been derived in similar ways

from other samples [e.g. Morganti et al. (1995) and references therein]. But the best-fit intrinsic prominences of jets are lower; $p_j \approx 0.005$ is a typical value derived from the fits for $\beta_j \approx 0.6$. In other words, even if the sources were not beamed, the sub-kpc-scale radio emission from the cores would be brighter than that from the much larger 100-kpc-scale jets. The beam is evidently much less efficient during the first few hundred pc of its journey to the hot spots than it is at any future time. This may be a sign either of strong interaction with the external medium or of shocks in the jet on these small scales, which would be consistent with a model in which the beam is decelerating strongly at this stage.

It is worth noting that the efficiency of the jet in these FRIIs is still very high; because the total radio luminosity of an extended source is much lower than the total power supplied by the beam (cf. Rawlings & Saunders 1991) and the unbeamed luminosity of the core and jet is less, by approximately $p_j + p_c$, than the total luminosity of the source, it follows that the efficiency of the jet is $\gg [1 - (p_j + p_c)]$, or probably > 99 per cent. Almost all the energy supplied by the beam is used to excite the lobe electron population and to do work on the external medium, and very little of it is radiated away in jets.

REFERENCES

Alef W., Wu S.Y., Preuss E., Kellermann K.I., Qiu Y.H., 1996, A&A, 308, 376

Barthel P.D., 1989, ApJ, 336, 606

Bowman M., Leahy J.P., Komissarov S.S., 1996, MNRAS, 279, 899

Bridle A.H., 1996, in Hardee P.E., Bridle A.H., Zensus J.A., eds, Energy Transport in Radio Galaxies and Quasars, ASP Conference Series vol. 100, San Francisco, p. 383

Bridle A.H., Hough D.H., Lonsdale C.J., Burns J.O., Laing R.A., 1994, AJ, 108, 766

Cawthorne T.V., 1991, in Hughes P.A., ed., Beams and Jets in Astrophysics, Cambridge University Press, Cambridge, p. 187

Fanaroff B.L., Riley J.M., 1974, MNRAS, 167, 31P

Fasano G., Francesini A., 1987, MNRAS, 225, 155

Garrington S., Leahy J.P., Conway R.G., Laing R.A., 1988, Nat, 331, 147

Hardcastle M.J., Alexander P., Pooley G.G., Riley J.M., 1996, MNRAS, 278, 273

Hardcastle M.J., Alexander P., Pooley G.G., Riley J.M., 1997, MNRAS, 288, L1

Hardcastle M.J., Alexander P., Pooley G.G., Riley J.M., 1998, MNRAS, 296, 445

Hough D.H., 1994, in Zensus J.A., Kellermann K.I., eds, Compact Extragalactic Radio Sources, NRAO workshop no. 23, NRAO, Green Bank, West Virginia, p. 169

Hughes P.A., Miller L., 1991, in Hughes P.A., ed., Beams and Jets in Astrophysics, Cambridge University Press, Cambridge, p. 1

Laing R.A., 1988, Nat, 331, 149

Laing R.A., 1996, in Hardee P.E., Bridle A.H., Zensus J.A., eds, Energy Transport in Radio Galaxies and Quasars, ASP Conference Series vol. 100, San Francisco, p. 241

Laing R.A., Jenkins C.R., Wall J.V., Unger S.W., 1994, in Bicknell G.V., Dopita M.A., Quinn P.J., eds, The First Stromlo Symposium: the Physics of Active Galaxies, ASP Conference Series vol. 54, San Francisco, p. 201

Laing R.A., Riley J.M., Longair M.S., 1983, MNRAS, 204, 151

LaValley M., Isobe T., Feigelson E.D., 1992, BAAS, 24, 839

Morganti R., Oosterloo T.A., Fosbury R.A.E., Tadhunter C.N., 1995, MNRAS, 274, 393

Peacock J.A., 1983, MNRAS, 202, 615

Press W.H., Flannery B.P., Teulolsky S.A., Vetterling W.T., 1992, *Numerical Recipes: The Art of Scientific Computing*, Cambridge University Press, Cambridge, 2nd ed

Preuss E., Alef W., Wu S.Y., Qiu Y.H., Qian Z.H., Kellermann K.I., Matveenko L., Götz M.M.A., 1990, in Zensus J.A., Pearson T.J., eds, Parsec-scale Radio Jets, Cambridge University Press, Cambridge, p. 120

Rawlings S., Saunders R., 1991, Nat, 349, 138

Ryle M., Longair M.S., 1967, MNRAS, 136, 123

Scheuer P.A.G., Readhead A.C.S., 1979, Nat, 277, 182

Spinrad H., Djorgovski S., Marr J., Aguilar L., 1985, PASP, 97, 932

Urry C.M., Padovani P., Stickel M., 1991, ApJ, 382, 501

Urry C.M., Schafer R.A., 1984, ApJ, 280, 569

Wardle J.F.C., Aaron S.E., 1997, MNRAS, 286, 425

Table 1. Fluxes and prominences for the sample sources

Source	Freq. (GHz)	Line class	Flux (Jy)	Error	Core flux (mJy)	Error	Core prom.	North jet Flux (mJy)	Error	South jet Flux (mJy)	Error	Brighter jet prominence
3C 15	8.35	E	1.00		28.00	0.05	0.04	96	3	< 1.4		0.1
3C 20	8.44	N	2.29		3.32	0.06	0.001	7	5	< 9		0.003
3C 33.1	1.53	B	3.02		20.40	0.07	0.02	< 37		27	4	0.007
3C 79	8.44	N	0.694		6.04	0.01	0.009	< 3.8		< 1.3		< 0.006
3C 98	8.35	N	3.08	0.07	6.1	0.1	0.002	50	20	< 13		0.02
3C 105	8.35	N	1.68		18.9	0.5	0.01	< 8.3		< 48		< 0.005
4C 14.11	8.44	E	0.500		29.69	0.03	0.06	< 0.45		1.14	0.04	0.002
3C 111	8.35	B	4.8	0.2	1276	1	0.4	90	20	< 58		0.03
3C 123	8.44	E	9.44		108.9	0.3	0.01	< 2.1		< 30		< 0.003
3C 132	8.44	E	0.674		4.1	0.2	0.006	< 13		2	3	0.004
3C 135	8.35	N	0.520		1.0	0.2	0.002	< 1.6		10	4	0.02
3C 136.1	8.35	?	1.00	0.05	1.53	0.03	0.002	< 2.6		< 2.7		< 0.003
3C 153	8.44	N	0.712		< 0.5		< 0.0007	8	1	13	5	0.02
3C 171	8.06	N	0.690		2.0	0.1	0.003	6.0	0.7	6.3	0.8	0.009
3C 173.1	8.44	E	0.461		9.64	0.02	0.02	2.1	0.9	< 0.29		0.005
3C 184.1	8.35	N	0.785		6.0	0.5	0.008	< 14		< 1.3		< 0.002
3C 192	8.35	N	1.38	0.08	4.0	0.2	0.003	< 3.2		< 7.7		< 0.002
3C 197.1	8.35	E	0.320		6.0	0.1	0.02	< 1.9		< 0.85		< 0.006
3C 219	4.87	B	2.27	0.06	51.6	0.1	0.04	56.5	0.3	2.1	0.1	0.03
3C 223	8.35	N	0.89	0.05	8.5	0.2	0.01	11	4	< 5.8		0.01
3C 223.1	8.35	N	0.53	0.01	6.4	0.4	0.01	3	1	< 21		0.006
3C 227	8.35	B	2.05	0.04	13.2	0.6	0.007	< 15		< 27		< 0.01
3C 234	8.44	N	0.919		34.46	0.04	0.04	10	8	< 19		0.01
3C 284	8.06	N	0.340		2.79	0.02	0.009	< 2.8		< 6.6		< 0.02
3C 285	4.86	N	0.740		6.8	0.4	0.02	19	2	< 14		0.03
3C 300	8.06	N	0.645		6.2	0.1	0.01	2.4	0.2	< 0.23		0.004
3C 303	1.48	B	2.45		106.6	0.3	0.2	63	5	< 13		0.03
3C 319	8.44	E	0.362		< 0.3		< 0.0008	< 0.12		< 1.8		< 0.005
3C 327	8.35	N	2.01	0.05	25	1	0.01	16	6	< 140		0.008
3C 349	8.44	N	0.723		24.21	0.02	0.03	< 0.053		0.31	0.04	0.0004
3C 353	8.44	E	14.1		151.0	0.2	0.01	70	10	< 34		0.005
3C 381	8.44	B	0.906		4.7	0.1	0.005	< 2.9		< 1.3		< 0.003
3C 382	8.35	B	1.30		251.2	0.1	0.2	14	1	< 1.1		0.01
3C 388	4.87	E	1.80		57.9	0.1	0.05	30	5	34	6	0.02
3C 390.3	8.35	B	2.8	0.1	733	5	0.4	20	10	< 650		0.008
3C 401	8.44	E	0.844		28.54	0.03	0.04	< 5.7		33.8	0.4	0.05
3C 403	8.35	N	1.50		7.1	0.2	0.005	6	1	< 3.8		0.004
3C 405	4.53	N	415		776	3	0.003	1200	600	500	800	0.003
3C 424	8.35	E	0.357		7.0	0.3	0.02	< 8.4		16.7	0.9	0.05
3C 433	8.35	N	2.08		1.2	0.3	0.0006	9.8	0.1	< 8.3		0.005
3C 436	8.44	N	0.592		17.90	0.02	0.03	< 0.27		3.8	0.8	0.007
3C 438	8.44	E	0.780		16.2	0.1	0.02	40	4	< 9.8		0.06
3C 445	8.40	B	1.34	0.08	83.9	0.4	0.07	< 1.9		14	3	0.01
3C 452	8.35	N	2.14		125.8	0.3	0.06	9	2	13	2	0.007

Column 2 gives the observing frequency of the radio data used in the analysis. Prominences are corrected to a nominal frequency of 8.4 GHz as described in paper I. Column 3 lists the emission line type of the source. 'E' indicates a LERG, 'N' a NLRG and 'B' a BLRG; '?' indicates an unclassified source. Paper I provides the references for these classifications. Column 4 gives the total flux density at the observing frequency. Errors on this quantity (column 5) are quoted only where the flux density was taken from the literature rather than VLA maps, or where there was some uncertainty in the definition of the source region on the VLA maps, as discussed in paper I; the standard VLA calibration errors apply to all other measured quantities.
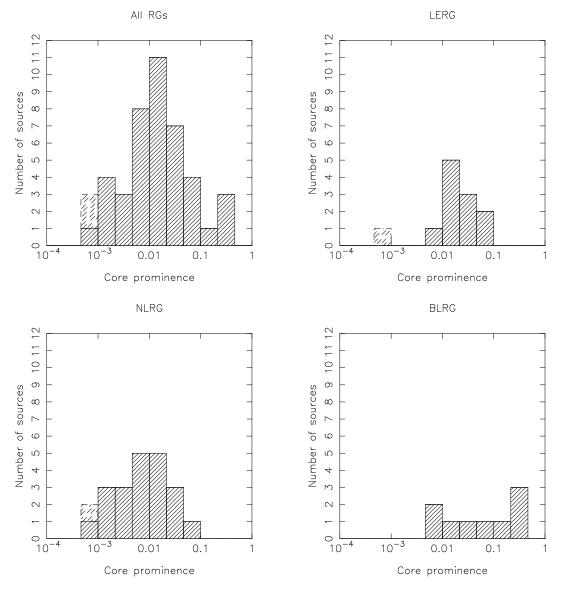
Figure 1. Core prominences of the objects in the sample classed by emission-line type. Dashed shading indicates an upper limit.
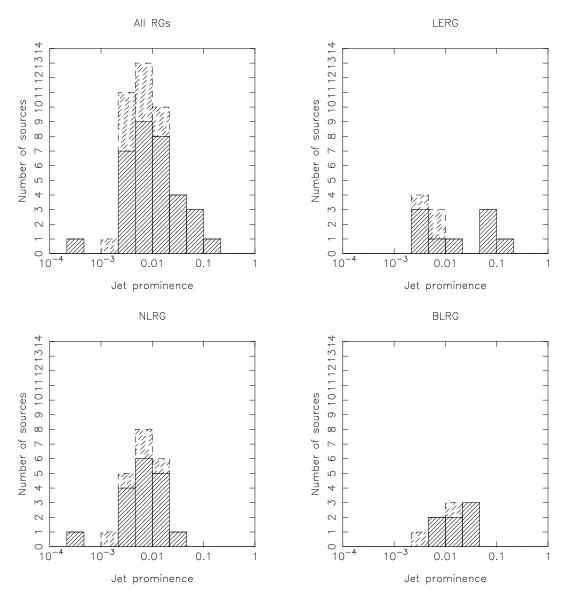
Figure 2. Jet prominences of the objects in the sample classed by emission-line type. Dashed shading indicates an upper limit.
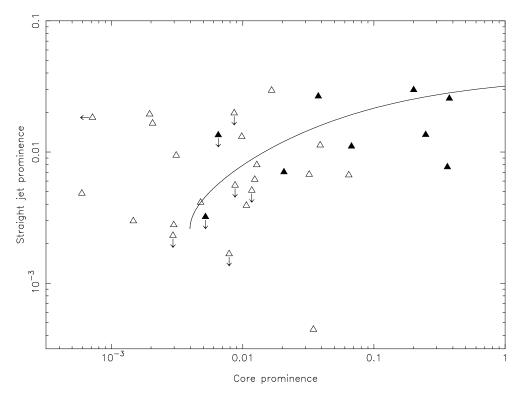
Figure 3. The relationship between core and jet prominences for the high-excitation objects in the sample. Filled symbols are BLRG, others are NLRG; arrows indicate upper limits. The solid line shows a theoretical curve assuming only relativistic beaming affects the prominences, using $\beta_j = 0.62$, $p_{\mathrm{j}} = 0.005$, $\beta_{\mathrm{c}} = 0.98$, $p_{\mathrm{c}} = 0.05$; see section 3.3.
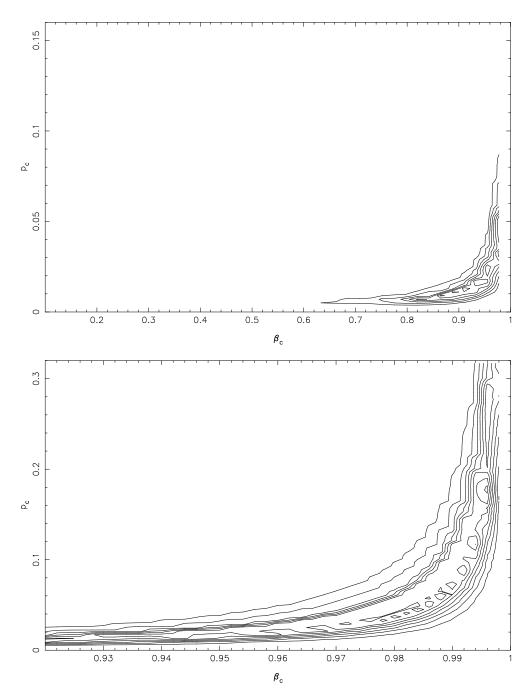
Figure 4. Kolmogorov-Smirnov probability contours for model core prominence data fitted to the prominences of BLRG and NLRG. Beaming speed β_c is plotted on the x-axis. Intrinsic prominence p_c is plotted on the y-axis. Contours at K-S probabilities of $0.05, 0.1, 0.15 \ldots, 0.40$. Above, β_c ranges from 0.1 to 0.98; below, as above but showing the region with $0.92 < \beta_c < 0.998$.
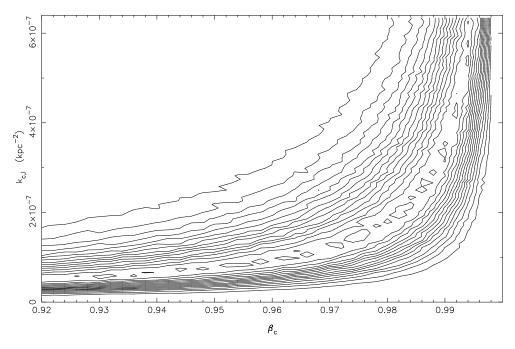
Figure 5. Kolmogorov-Smirnov probability contours for model core prominence data fitted to the prominences of BLRG and NLRG, including a dependence of intrinsic prominence on source length as discussed in the text. Beaming speed β_c is plotted on the x-axis, and varies between 0.92 and 0.998; the constant relating length to intrinsic prominence, $k_{c,l}$ (kpc $^{-2}$), is plotted on the y-axis. Contours at K-S probabilities of $0.05, 0.1, 0.15 \ldots, 0.75$.
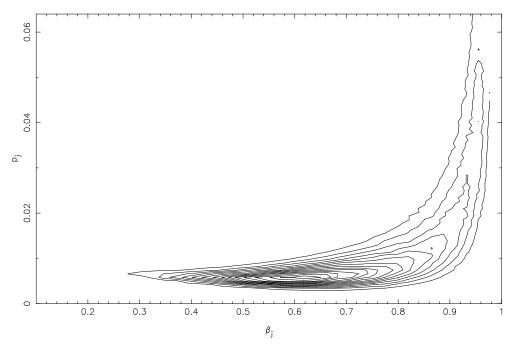

Figure 6. Kolmogorov-Smirnov probability contours for model jet prominence data fitted to the prominences of BLRG and NLRG. Beaming speed β_j is plotted on the x-axis, and varies between 0.1 and 0.98; intrinsic prominence p_j is plotted on the y-axis. Contours at K-S probabilities of $0.05, 0.1, 0.15 \ldots, 0.70$.